IDENTIFICATION OF IMPEDANCE SOURCES RESPONSIBLE FOR LONGITUDINAL BEAM INSTABILITIES IN THE CERN PS

A. Lasheen*, H. Damerau, G. Favia, P. Kozlowski, B. Popovic,
CERN, Geneva, Switzerland

Abstract

Longitudinal instabilities in the CERN PS are an important limitation to obtain the expected beam intensity and longitudinal emittance at the PS extraction in the framework of the LHC Injector Upgrade (LIU) project. The observed coupled-bunch instabilities lead to dipolar and quadrupolar oscillations, as well as to an uncontrolled longitudinal emittance blow-up for proton beams. A microwave instability observed with ion beams develops quickly at transition crossing. To identify the potential impedance sources of these instabilities, two strategies were adopted. Firstly, beam measurements were performed for different impedance configurations, i.e. by partially detuning the main RF cavities. Secondly, a thorough survey of the machine elements together with the RF studies allowed to refine the PS impedance model in order to find potentially missing contributions. Measurements were compared with particle simulations using the updated impedance model of the PS. Although the source of the dipolar coupled-bunch instability was already identified in the past, this study led to an identification of the impedance sources driving other types of longitudinal instabilities.

INTRODUCTION

An important objective of the High Luminosity-LHC (HL-LHC) project at CERN is to double the beam (and bunch) intensity [1]. This target intensity is challenging for the injectors, which are being upgraded in the framework of the LHC Injector Upgrade (LIU) project [2]. The Proton Synchrotron (PS) is the second synchrotron in the injector chain and it accelerates the proton beam up to $p = 26$ GeV/c before extraction to the Super Proton Synchrotron (SPS). The present nominal intensity of LHC-type beams extracted from the PS is $N_p = 1.3 \times 10^{11}$ protons per bunch (p/b), and the LIU target is $N_p = 2.6 \times 10^{11}$ p/b with the same longitudinal emittance. Main limitations in the PS to reach these parameters are longitudinal beam instabilities.

Before the LIU upgrades, the dipolar coupled-bunch instability was the most critical instability in the PS, with a threshold close to the nominal LHC-beam intensity. Using analytical studies and particles simulations [3], its impedance source was identified to be the fundamental impedance of the main RF system (10 MHz ferrite-loaded cavities). In the framework of the LIU project, a dipolar coupled-bunch feedback was developed and successfully implemented as mitigation measure, allowing to raise the beam intensity up to $N_p = 2.3 \times 10^{11}$ p/b. Although close to the target intensity, the goal was not yet reached due to other intensity effects.

* alexandre.lasheen@cern.ch

The quadrupolar coupled-bunch instability, which is not damped by the dipolar coupled-bunch feedback, limits the beam from reaching the parameters required for the LIU project. This instability was mitigated before, even without understanding the driving impedance source, by using one of the 40 MHz cavity as a Landau RF system [4]. This provided the stability margin allowing to achieve beam parameters beyond the LIU target. Although the required longitudinal beam parameters were reached in the PS, the impedance source driving the quadrupolar coupled-bunch instability was yet to be identified. In this paper, we start from an overview of the present PS impedance model including the latest identified sources. Next, we describe the limitations other than coupled-bunch instabilities for which the driving impedance sources were already identified. Finally, the main focus of this paper is to describe the methods used to identify the impedance source responsible for the quadrupolar coupled-bunch instability.

PS BEAM-COUPLING IMPEDANCE MODEL

The present PS impedance model, shown in Fig. 1, was developed over the course of several years. The model is based on electromagnetic simulations, as well as beam measurements of the impedance [5] and includes [6]

- RF systems (with frequencies 2.8-10, 20, 40, 80, 200 MHz, and a broadband Finemet system);
- kicker magnets (injection/extraction, 6 elements);
- vacuum equipment (pumping manifolds, bellows, sector valves);
- longitudinal space charge and beam pipe resistive wall impedance;
- single elements, such as internal beam dumps, beam pick-ups.

Although not all different versions of the equipment are included (e.g. all possible variations of the pumping manifolds), the most relevant elements are present in the model. The principal impedance sources driving the instabilities are therefore expected to be in the list of elements.

The impedance sources have different effects depending on their wavelength-to-bunch length ratio given by the parameter $f_r\tau$ where f_r is the resonant frequency of the impedance and τ the bunch length. The contributions at low frequencies, $f_r\tau \sim 1$ ($\lesssim 40$ MHz in Fig. 1), are expected to drive dipole and quadrupole coupled-bunch instabilities, while high frequency sources, $f_r\tau \gg 1$ ($\gg 40$ MHz), are

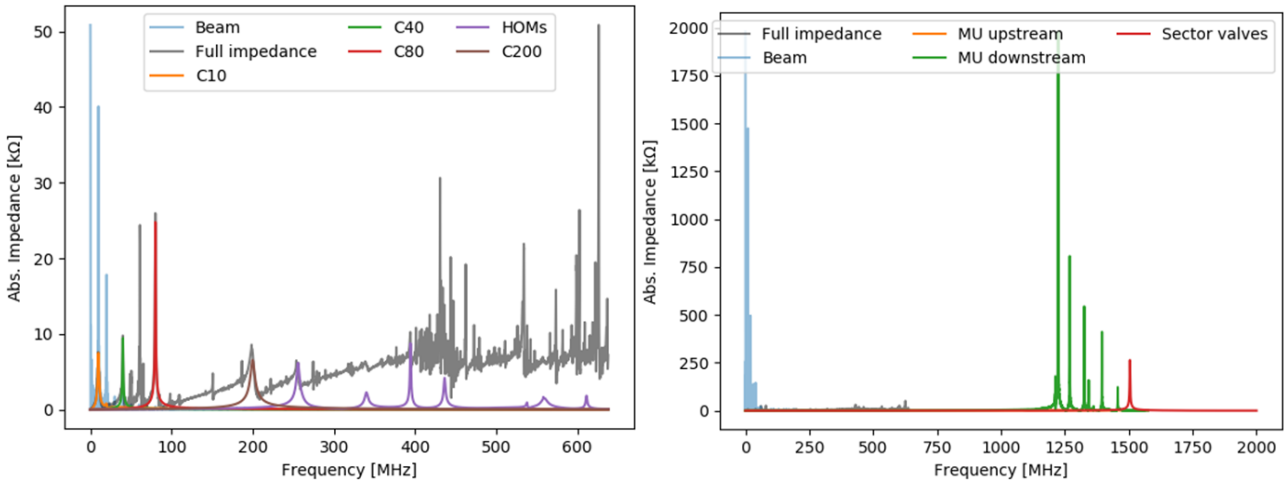

Figure 1: Absolute value of impedance versus frequency for the present PS impedance model. The cavity impedances are labeled with a 'C' followed by their resonant frequency. The equipment around the main magnet units (MU) consists of bellows upstream and pumping manifolds downstream. These also house pick-ups of the trajectory measurement system. The kicker magnets are not labeled but contribute to the broadband impedance. The beam spectrum is displayed in blue (in arbitrary units) to illustrate which contributions are considered to be low frequency, $f_r\tau \sim 1$, and high frequency, $f_r\tau \gg 1$.

expected to drive microwave instability leading to uncontrolled emittance blow-up. The broadband impedances can also lead to loss of Landau damping.

IDENTIFIED LIMITATIONS

One of the limiting intensity effects in the PS was an uncontrolled emittance blow-up arising during the acceleration ramp and the beam splittings at top energy. The source of the instability was rapidly identified as the high frequency RF system (80 MHz cavities). Three of these cavities are installed in the ring, but only two are required for proton operation (non-adiabatic bunch shortening before extraction to the SPS). When not in use, the cavity impedance is shielded from the beam by closing the gap with a pneumatic short-circuit. The contribution to the uncontrolled emittance blow-up of these cavities was brought to light by comparing the longitudinal beam quality with the 80 MHz cavity gaps opened and closed. Another applied technique consisted in measuring the beam spectrum during the slow debunching with RF off [7]. An example of measured beam profile and spectrum is shown in Fig. 2. The uncontrolled emittance blow-up was removed using a multi-harmonic RF feedback to reduce the impedance of the high frequency cavities, as demonstrated in [8], allowing to reach the LIU beam intensity at the nominal longitudinal emittance.

Another potential source of uncontrolled emittance blow-up is the microwave instability cause by the very high frequency impedance sources. Presently it has no critical impact on proton beam operation. However, for the ion beam, the microwave instability occurs right after transition crossing, as illustrated in Fig. 3. The frequency analysis of the bunch profile allowed to have an indication of the frequency of the driving impedance source [9]. However, short bunches are not ideal for these measurements and

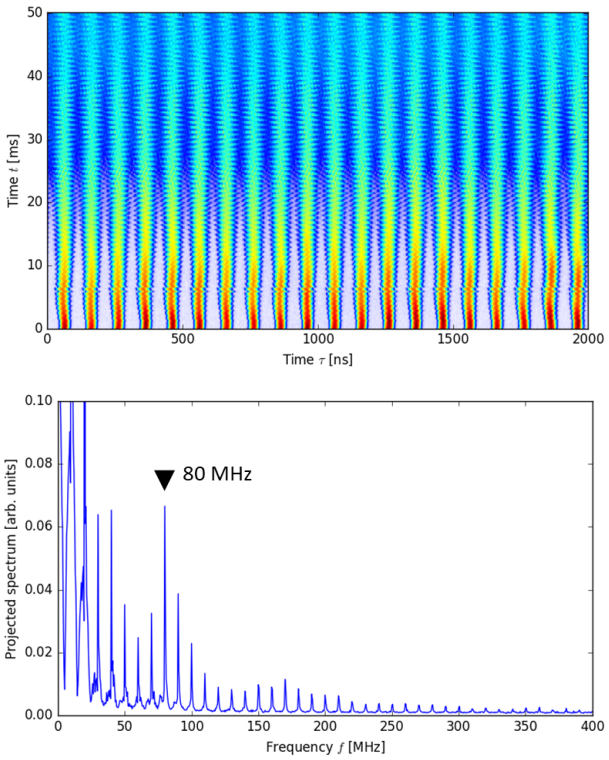

Figure 2: Measurement of beam modulation by the 80 MHz cavities impedance during adiabatic reduction of the RF voltage. The profiles (top) are shown with the corresponding projected spectrum (bottom, maximum spectral amplitude).

only provide poorly resolved information about the resonant frequency of the impedance, in the frequency range above 1 GHz. Empty pumping manifolds are the suspected main impedance source at high frequency and were already

considered in 1975 [10], when damping resistors were installed. Although not critical for proton beam operation, these sources of impedance need to be carefully monitored as they might be responsible for the generation of tails in the longitudinal distribution. This could lead to losses during PS-SPS transfer [11], as well as to high frequency structures on the extracted bunch profile.

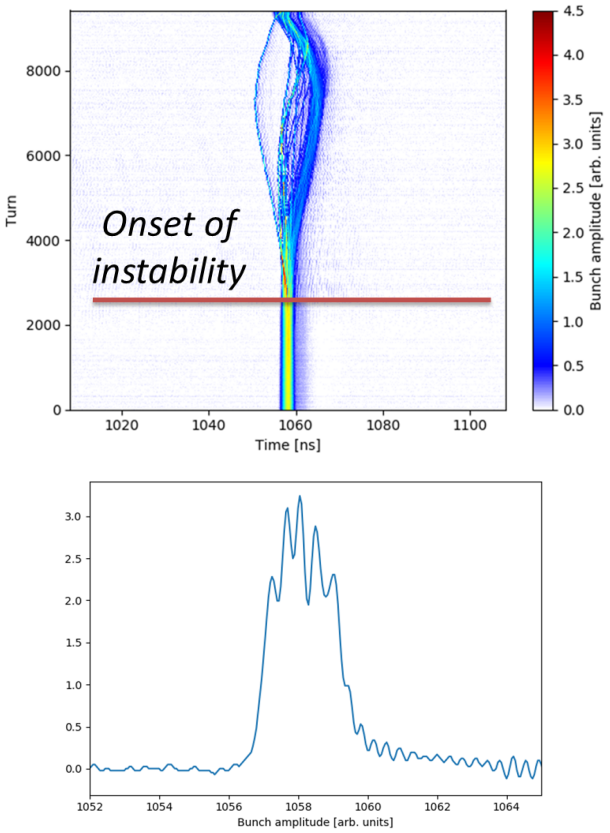

Figure 3: Microwave instability at transition crossing with ion beam ($^{208}Pb^{54+}$). The evolution of the bunch profile (top) is shown together with the one right after the onset of the instability (bottom), where the profile is modulated by beam induced voltage due to high frequency impedance sources (> 1 GHz).

MEASUREMENTS AND ANALYSIS OF THE QUADRUPOLAR COUPLED-BUNCH INSTABILITY

The beam in the PS is accelerated using ferrite-loaded cavities, tuneable from 2.8 MHz to 10 MHz. During the acceleration ramp, the cavities are tuned at $h = 21$ (about 10 MHz) and follow the RF voltage program shown in Fig. 4. For the nominal beam, $n_b = 18$ bunches are accelerated. On the arrival to the flat top, the RF voltage is adiabatically reduced to $V_{\mathrm{RF}} = 20$ kV and the bunches are split four times before being compressed and extracted to the SPS. The RF voltage during the ramp is distributed over 10 cavities, each of them being composed of 2 gaps. One extra cavity is installed in the ring as a spare. The cavities are distributed in 3 groups (A,B,C) sharing the same bias tuning current and 4 voltage program groups (1,2,3,4, different shades of purple in Fig. 4). Each RF gap of the cavities is equipped with a relay to short-circuit the gap and to minimize the beam-coupling impedance, when not in use, independently for each voltage program group. Unused cavities can also be 'parked' by tuning them to a low, non-integer harmonic number (e.g. $h = 6.5$). This slightly reduces the impedance with closed gap relays, independently for each tuning group.

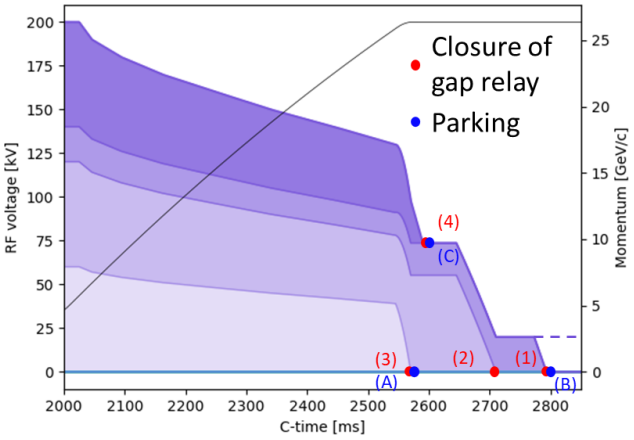

Figure 4: Momentum (black) and RF voltage (purple) programs as a function of time during the acceleration ramp, starting at transition crossing. During coupled-bunch instability studies, the beam splitting process at the flat-top is disabled and the RF voltage is kept at $V_{\mathrm{RF}} = 20$ kV till the end of the cycle (dashed line).

The coupled-bunch instabilities (dipolar and quadrupolar), usually occuring at top energy, can also be observed during the ramp for high intensities or smaller longitudinal emittances. An example of such instability is shown in Fig. 5. In this particular example, a full ring with $n_b = 21$ bunches in $h = 21$ was accelerated for easier mode analysis. Each bunch oscillates with an amplitude A_b, at the frequency $m\omega_s$ (where $f_s = \omega_s/(2\pi)$ is the synchrotron frequency) and a phase ϕ_b. The coupling between the bunches can be analyzed using the expression

$$A_\mu \sin\left(m\omega_s t + \phi_\mu\right) = \frac{1}{n_b}\sum_{b=0}^{n_b-1} A_b \sin\left(m\omega_s t + \phi_b - \frac{2\pi b\mu}{n_b}\right), \quad (1)$$

where b is the bunch index, μ is the mode number, A_μ is the mode amplitude and ϕ_μ the mode phase. The Eq. (1) corresponds to the spectral analysis of the bunch oscillations based on a discrete Fourier transform, assuming that all bunches oscillate with the same synchrotron frequency. In practice, the bunch position oscillations are analyzed to get the dipolar mode spectrum $m = 1$ and bunch length oscillations for quadrupolar mode spectrum $m = 2$.

Results from measurements performed with $n_b = 18$ bunches at the LIU intensity of $N_p = 2.6 \times 10^{11}$ p/b

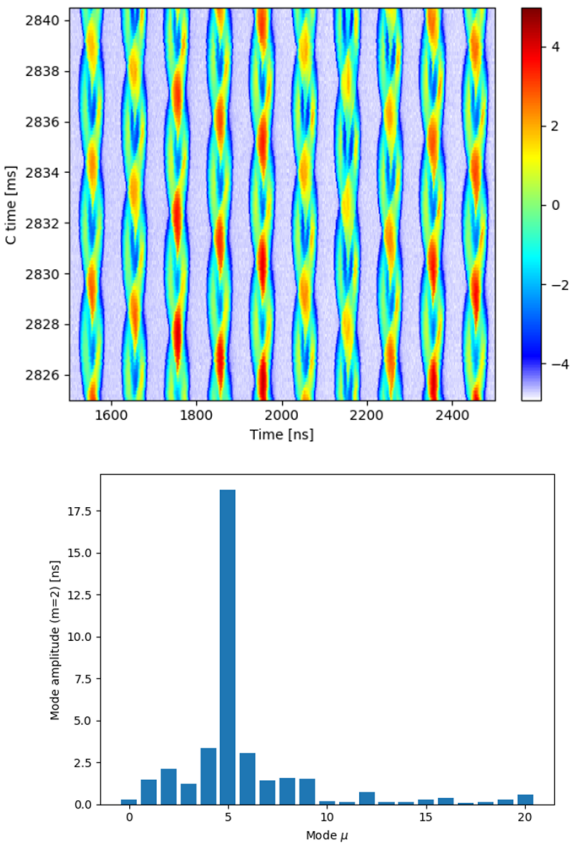

Figure 5: Example of measured bunch profiles undergoing quadrupolar coupled-bunch oscillations (top, color scale in arbitrary units) with the corresponding mode spectrum of the bunch length oscillations using Eq. (1). The dominant mode is $\mu_{n_b=21} = 5$ (i.e. every 5$^{\text{th}}$ bunch oscillates in phase).

at extraction are shown in Fig. 6. In this set of measurements, the longitudinal emittance was scanned by varying the amplitude of the controlled emittance blow-up (phase modulation of a very high harmonic RF system at 200 MHz, 6 cavities). The nominal blow-up setting 3x4.5 kV yields a longitudinal emittance at extraction of $\varepsilon_l = 0.35$ eVs. Reducing the blow-up setting down to 3x0.5 kV decreases the longitudinal emittance by about 20%. The amplitude of the oscillations stays reasonably small for the nominal longitudinal emittance, but rapidly increases when reducing the emittance by a few percents.

Systematic measurements of coupled-bunch instabilities during the Run 2 (2013-2018) were conducted and lead to reproducible results. One of the remarkable results is that the dominant oscillation modes μ always remained identical with $n_b = 18$: $\mu_{n_b=18} = [1, 2]$ during the acceleration ramp and $\mu_{n_b=18} = [4, 5]$ at top energy, both for dipolar $m = 1$ and quadrupolar $m = 2$ instabilities. This information is essential to identify the impedance source driving the instability.

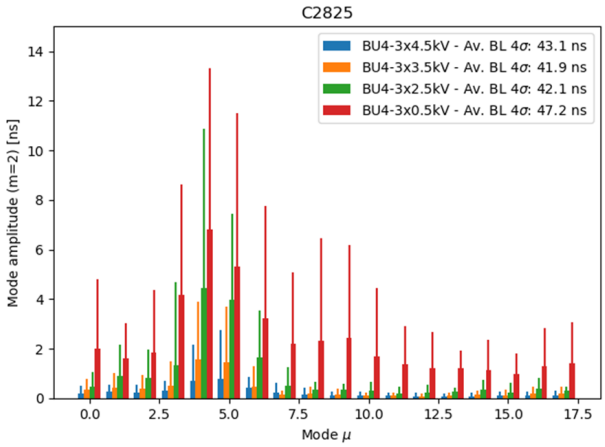

Figure 6: Mode spectrum of quadrupolar oscillations for various longitudinal emittances. The emittance is set by the controlled emittance blow-up (BU) during the ramp. The error bars correspond to the maximum amplitude spread measured over 10 cycles. The average bunch length is given at extraction, and it is larger for the smallest blow-up setting (red) due to the beam instability.

IDENTIFICATION AND EXPERIMENTAL CONFIRMATION OF THE IMPEDANCE SOURCE

First estimates of the characteristics of the impedance responsible for quadrupolar coupled-bunch instabilities were done analytically.

Unstable Synchrotron Frequency Side-bands

To drive the instability in the case of a ring filled with equidistant bunches, an impedance source must cover a synchrotron frequency side-band of the beam spectrum given by

$$f_{n,\mu} = (nh + \mu)\, f_0 + m f_s, \tag{2}$$

where $n \in \mathbb{N}$ is the revolution mode number. In the case of the PS, where bunches are partially filling the ring, the expression can be approximated by

$$f_{n,\mu} = \left(nh + \left\lfloor \mu \frac{h}{n_b} \right\rceil\right) f_0 + m f_s, \tag{3}$$

where $\lfloor \cdot \rceil$ denotes the rounding to the nearest integer value, and μ is obtained from the mode analysis in Eq. (1) on the actual number of bunches n_b. For example, the mode $\mu_{n_b=21} = 5$ obtained with $n_b = 21$ bunches (Fig. 5) corresponds to the mode $\mu_{n_b=18} = 4$ obtained with $n_b = 18$ bunches (Fig. 6) and they both are excited by an impedance source at a fixed frequency.

The first condition defines possible frequencies of the impedance source responsible for the instabilities. For low values of $\mu = [1, 2]$, the driving impedance source is expected to be not further than approximately 1 MHz above the main RF harmonics (the revolution period is $f_0 \approx 477$ kHz

at top energy in the PS). This is the case for the RF systems, in particular the 10 MHz RF cavities with a bandwidth large enough to cover modes $\mu_{n_b=18} = [1, 2]$ and it was shown to be the source of dipolar coupled-bunch instability [3]. For the larger values of $\mu_{n_b=18} = [4, 5]$, the impedance is expected to be around 2.5 MHz above the main RF frequency on its harmonic, which is beyond the bandwidth of the RF cavities. Two assumptions can be made: Another source of impedance should hence be suspected, or the resonant frequency of the same impedance source is changing and drives both instabilities during the ramp and at flat-top energy.

Threshold in Shunt Impedance vs. Frequency

A limitation of the criterion used above is that, due to the sampling with the bunch frequency, the impedance source is expected to be at a resonant frequency of $f_{n,\mu}$, but for any n. To further restrict the possible frequency range and the amplitude of the impedance, another criterion can be obtained from the shunt impedance threshold for coupled-bunch instabilities given by [12]

$$R_s < \frac{|\eta|\, E}{e I_0 \beta^2} \left(\frac{\Delta E}{E}\right)^2 \frac{\Delta\omega_s}{\omega_s} \frac{F}{f_0 \tau} G\left(f_r \tau\right), \qquad (4)$$

where $\eta = \gamma_{\mathrm{tr}}^{-2} - \gamma^{-2}$ is the slippage factor, E the beam energy, e the elementary charge, I_0 the average beam current, β the relativistic velocity factor, $\Delta E/E$ the energy spread, $\Delta\omega_s/\omega_s$ the synchrotron frequency spread, $F \sim 0.3$ a form factor defined by the particle distribution and G is a form factor defined as

$$G\left(x\right) = x \min\left\{J_m^{-2}\left(\pi x\right)\right\}. \qquad (5)$$

where J_m is the Bessel function of the first kind and min denotes the minimum value over all modes m.

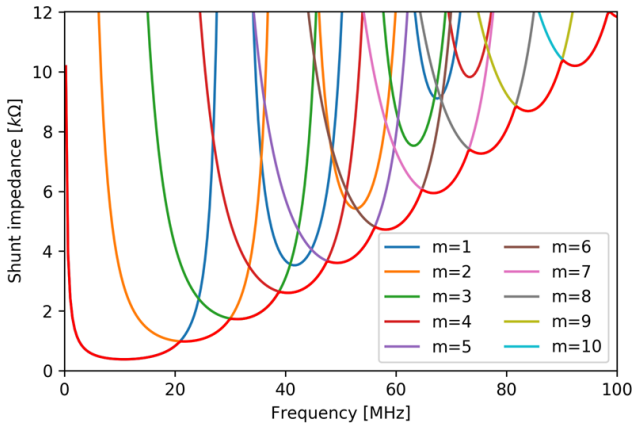

Figure 7: Shunt impedance threshold for coupled-bunch instabilities according to Eq. (4) up to mode $m = 10$. The red line corresponds to the minimum of all modes m considered.

Applying Eq. (4) to beam parameters on the PS flat top provides the curves shown in Fig. 7. The instability threshold depends on the wavelength-to-bunch length ratio $f_r\tau$. For the dipolar mode $m = 1$, the required shunt impedance is minimum in the region around 10 MHz (compatible with the observation that the main RF system is responsible for dipolar instabilities), while for the quadrupolar mode $m = 2$ the required shunt impedance is minimum in the region around 20 MHz. Combining both criteria, the most likely impedance source for quadrupolar instabilities has a resonant frequency of about 22.5 MHz and a minimum shunt impedance, R_s of about 1 kΩ.

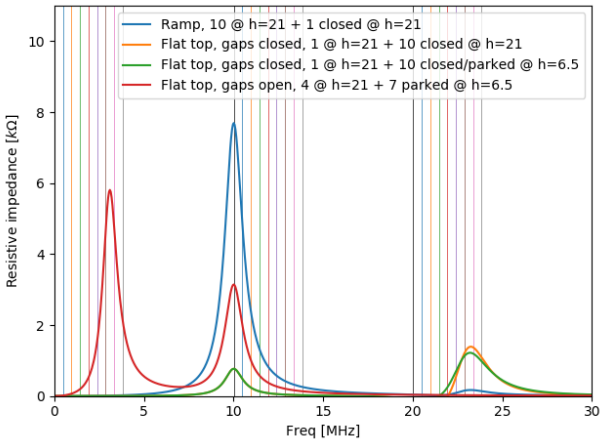

Figure 8: Impedance of the 10 MHz cavities (11 in total) for different configurations. The frequency of the unstable modes according to Eq. (3) with $n_b = 21$ bunches are displayed as vertical lines.

Using the present PS impedance model, the closest impedance source with the expected characteristics are therefore the 10 MHz cavities when the gap relay is closed. The gap relay is not perfect and this contribution, which was assumed negligible in the past, should be included in the model. Indeed, the shunt impedance of the cavity with closed gap is $R_s \approx 70\ \Omega$ per gap at a resonant frequency of $f_r \approx 23.1$ MHz [13]. During the ramp, the voltage program of all the cavities except one is reduced to zero, immediately followed by the closure of the gap relays and parking to $h = 6.5$ (see Fig. 4). Although small, the residual impedance of all cavities is summed up and amounts to an impedance of $R_s \approx 1.4$ kΩ, as shown in Fig. 8 (blue line during the ramp, orange line at flat top). Note that changing the tuning current of the cavity with the gap relay closed has no major influence on its impedance (green line in Fig. 8). A final point is that the impedance of the 10 MHz cavities changes along the ramp, which explains the observation that the mode μ changes from the acceleration ramp to the flat-top. Overall, the impedance of the 10 MHz cavities, including their residual impedance when the gap relays are closed, fulfills all the conditions to explain the behavior of both dipolar and quadrupolar coupled-bunch instabilities.

Experimental Verification

Additional measurements were therefore conducted to validate this hypothesis experimentally. The test consisted of measuring the quadrupolar coupled-bunch instabilities

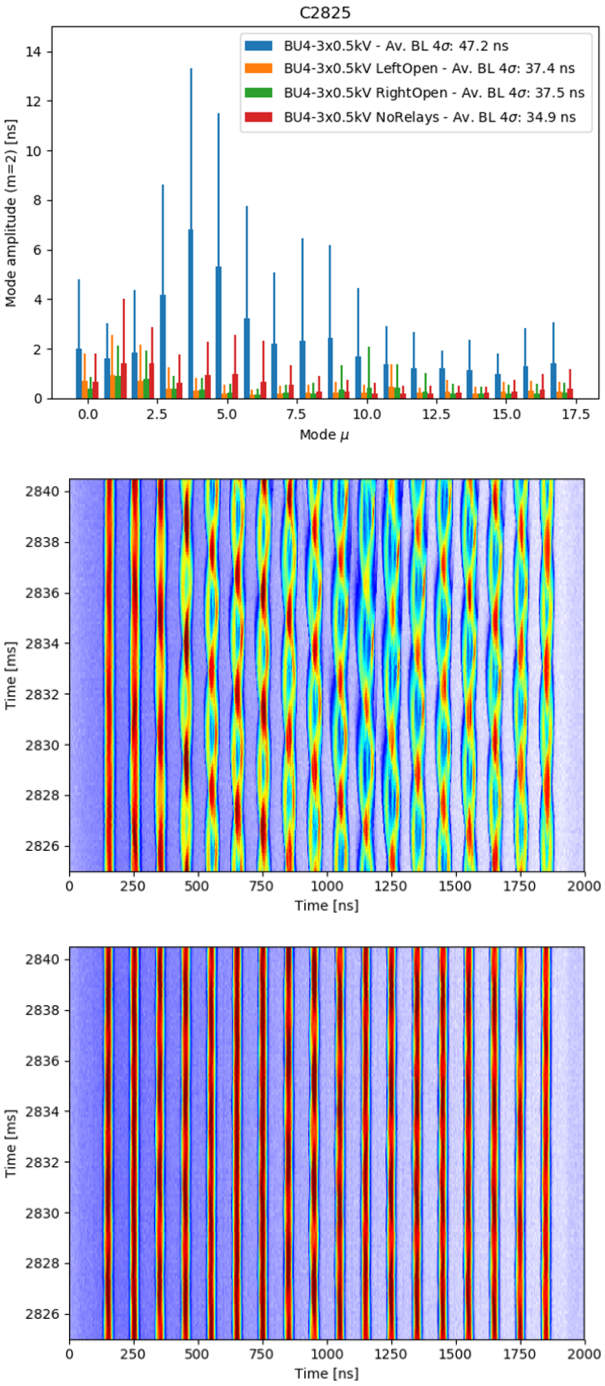

Figure 9: Quadrupolar mode spectrum with $n_b = 18$ bunches for different 10 MHz cavities impedance configurations (top). The bottom plots show the measured beam profiles with the gap relays closed (middle) and opened with the cavities parked to $h = 6.5$ (bottom).

with different configurations of the 10 MHz cavities. Note that the longitudinal emittance was set to the lowest possible value (with the BU setting at 3x0.5 kV) in order to provoke the instability. Furthermore, note that the dipolar coupled-bunch feedback was kept enabled. To confirm the fact that the impedance at 23 MHz is responsible for the quadrupolar instabilities, the gap relays of cavities were blocked opened. Unused cavities belonging to the same harmonic group were parked at $h = 6.5$ with their impedance at the fundamental resonance affecting the beam. In this case, all impedance contributions are far from the parameter region driving quadrupolar instabilities, as shown in red in Fig. 8. Even though the overall impedance is much larger with the gap relays opened, it is expected that in this frequency range the impedance should drive dipolar instabilities, which are damped by the coupled-bunch feedback.

The results are summarized in Fig. 9. The amplitude of quadrupolar oscillations is drastically reduced by moving the impedance far away from the critical region around 20 MHz, confirming all hypotheses above. Note that the average bunch length at extraction is smaller for the case with the gap relays open, which is an indication that the beam is simply not stabilized by any other source of emittance blow-up occurring before the quadrupolar instability could rise. The residual impedance of the cavities with closed gap relays can therefore be assumed responsible for the quadrupolar coupled-bunch instabilities of modes $\mu_{n_b=18} = [4, 5]$. An immediate question is whether it is possible to profit from this observation in operation. Unfortunately, detuning the impedance to very low frequency triggers other effects, like degradation of the RF manipulations due to transient beam loading. An example of bunch-by-bunch variation with and without the gap relays is shown in Fig. 10, where the first bunch is too large to be extracted to the SPS without losses. Possible improvements of the gap relay circuit or other measures to reduce the impedance of the spurious resonance at 23 MHz are therefore being considered.

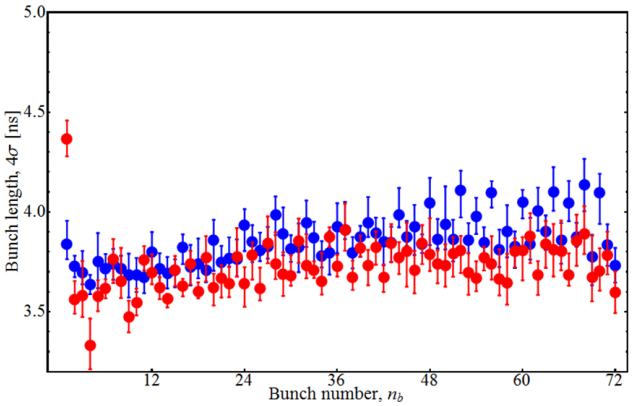

Figure 10: The bunch length at PS extraction with opened and closed gap relays. The case with the gap relays opened was obtained with the cavities parked at $h = 6.5$. The source of degradation of the longitudinal emittance of the first bunch only remains to be identified.

CONCLUSIONS

The development of the PS longitudinal impedance model makes progress by combining efforts of modeling the devices

in the machine, but also by performing beam-based measurements of the impedance. The main impedance sources responsible for longitudinal instabilities are mostly identified or have clear suspects:

- The 80 MHz cavities are responsible for uncontrolled blow-up during splitting.
- High frequency impedance sources (e.g. pumping manifolds, sector valves) are suspected to drive the microwave instability at transition crossing for ions.
- The 10 MHz cavities with closed gap relay have a resonance at about 23 MHz responsible for the quadrupolar coupled-bunch instability at flat top.

Further work will consist in improving the analytical estimations in order to evaluate the evolution of the instability threshold along the ramp, including the variations on bunch length. Moreover, the criterion used in [12] provides pessimistic values and the criterion presented in [14] should provide more accurate results. Progress in particle simulations is also ongoing and will require an accurate modeling of feedbacks to reproduce all measured instabilities.

ACKNOWLEDGMENTS

We would like to thank the PS operators for their support during MD sessions, colleagues from the RF-IS section for their help with measurements of cavities impedance, as well as all contributors to the PS impedance model.

REFERENCES

[1] G. Apollinari, I. Béjar Alonso, O. Brüning, P. Fessia, M. Lamont, L. Rossi, and L. Tavian, "High-Luminosity Large Hadron Collider (HL-LHC): Technical Design Report V. 0.1," Tech. Rep. CERN-2017-007-M, Geneva, 2017.

[2] H. Damerau, A. Funken, R. Garoby, S. Gilardoni, B. Goddard, K. Hanke, A. Lombardi, D. Manglunki, M. Meddahi, B. Mikulec, G. Rumolo, E. Shaposhnikova, M. Vretenar, and J. Coupard, "LHC Injectors Upgrade, Technical Design Report, Vol. I: Protons," Tech. Rep. CERN-ACC-2014-0337, CERN, Geneva, Switzerland, 2014.

[3] H. Damerau, S. Hancock, C. Rossi, E. N. Shaposhnikova, J. Tuckmantel, J. L. Vallet, and M. Mehler, "Longitudinal Coupled Bunch Instabilities in the CERN PS," in *Particle accelerator. Proceedings, 22nd Conference, PAC'07, Albuquerque, USA, June 25-29, 2007*, vol. C070625, p. 4180, 2007.

[4] H. Damerau, A. Lasheen, and M. Migliorati, "Observation and Damping of Longitudinal Coupled-bunch Oscillations in the CERN PS," *CERN Yellow Rep. Conf. Proc.*, vol. 1, pp. 33–37. 5 p, 2018.

[5] M. Migliorati, S. Persichelli, H. Damerau, S. Gilardoni, S. Hancock, and L. Palumbo, "Beam-wall interaction in the cern proton synchrotron for the lhc upgrade," *Phys. Rev. ST Accel. Beams*, vol. 16, p. 031001, 2013.

[6] "PS Longitudinal Impedance Database." https://gitlab.cern.ch/longitudinal-impedance/PS/.

[7] A. Lasheen, H. Damerau, and G. Favia, "Uncontrolled longitudinal emittance blow-up during rf manipulations in the CERN PS," *Journal of Physics: Conference Series*, vol. 1067, p. 062018, 2018.

[8] H. Damerau, F. Bertin, G. Favia, and A. Lasheen, "Active methods of suppressing longitudinal multi-bunch instabilities," in *these proceedings*.

[9] T. Bohl, T. P. R. Linnecar, and E. Shaposhnikova, "Measuring the resonance structure of accelerator impedance with single bunches," *Phys. Rev. Lett.*, vol. 78, pp. 3109–3112, 1997.

[10] D. Boussard, "Observation of microwave longitudinal instabilities in the CPS," Tech. Rep. CERN-LabII-RF-INT-75-2. LabII-RF-INT-75-2, CERN, Geneva, Switzerland, 1975.

[11] A. Lasheen, H. Damerau, J. Repond, M. Schwarz, and E. Shaposhnikova, "Improvement of the Longitudinal Beam Transfer from PS to SPS at CERN," in *Proc. 9th International Particle Accelerator Conference (IPAC'18), Vancouver, BC, Canada, April 29-May 4, 2018*, no. 9 in International Particle Accelerator Conference, (Geneva, Switzerland), pp. 3060–3063, JACoW Publishing, 2018. https://doi.org/10.18429/JACoW-IPAC2018-THPAF042.

[12] E. Shaposhnikova, "Longitudinal beam parameters during acceleration in the LHC," Tech. Rep. LHC-PROJECT-NOTE-242, CERN, Geneva, Switzerland, 2000.

[13] G. Favia, "Study of the beam-cavity interaction in the CERN PS 10 MHz cavities and investigation of hardware solutions to reduce beam loading," no. CERN-THESIS-2017-166, 2017.

[14] I. Karpov and E. Shaposhnikova, "Longitudinal Coupled-Bunch Instability Evaluation for FCC-hh," in *Proc. 10th International Particle Accelerator Conference (IPAC'19), Melbourne, Australia, 19-24 May 2019*, no. 10 in International Particle Accelerator Conference, (Geneva, Switzerland), pp. 297–300, JACoW Publishing, Jun. 2019. https://doi.org/10.18429/JACoW-IPAC2019-MOPGW083.